Mixed evaporite/carbonate characteristics of the Triassic Kangan Formation, offshore area, Persian Gulf

Akbar Zamannejad[1,*], Davood Jahani[1], Masoud Lotfpour[2], and Bahram Movahed[3]

[1] Department of Geology, Faculty of Sciences, North Tehran Branch, Islamic Azad University, No. 91, South Makran St., Pasdaran Ave. , P.O. Box 19585-851, Tehran, Iran.
[2] Head of Reservoir Geology Department, Tehran Energy Consultants (TEC), No.6, 2nd Alley, Arabali St., Khoramshar Ave., P.O.Box15546, Tehran, Iran.
[3] Head of Geology and Petrophysics Department, Dana Oil and Gas Energy Company, No.140, Zafar Ave, P.O. Box 1919935-331, Tehran, Iran.
** azamannejad19@yahoo.com*

ABSTRACT

The Early Triassic Kangan Formation is a mixed carbonate-evaporite succession that is considered to be part of the largest carbonate gas reservoir in the Persian Gulf region. This stratigraphic succession is characterized by alternating limestone, dolostone, evaporite and shale that have been investigated in terms of evaporite facies characteristics in the Iranian offshore area. The main body of Kangan carbonates was deposited in a shallow-marine, restricted carbonate ramp platform, and underwent intense near-surface diagenesis and minor burial modification. Evaporitic facies consist of anhydrite, secondary anhydrite after gypsum, and mixed carbonate-evaporite, which are dominant in the different parts of Kangan Formation, as result of arid climate and abrupt eustatic sea level changes. This article focuses on the evaporite successions, in which diverse evaporitic lithofacies have been recognized that can be categorized in two main classes: (1) carbonate-dominated facies with evaporite contents (C facies types), and (2) evaporite-dominated with minor carbonate contents (A facies types). Fine-crystalline anhydrite laminae and bands, bedded evaporite (bedded pseudomorphs); interstitial anhydrite pseudomorphs after gypsum and nodular anhydrite are common features. The evaporite successions in microscopic and macroscopic scales indicate that dolomitization and anhydrite precipitation took place contemporaneously, as ascribed to sabkha/seepage-reflux models. The evaporite sedimentation has mainly occurred in a subsiding coastal basin of a salina or hypersaline lagoon. In this setting, the subaqueous precipitation of the carbonate and evaporite lithofacies was followed by the interstitial growth of diagenetic, secondary anhydrite. As a whole, the evaporite succession reflects an infilling and diagenetic process. Gypsum was converted to anhydrite pseudomorphs following shallow to deep burial diagenesis events.

Key words: evaporite, anhydrite, Kangan Formation, Triassic, Persian Gulf, Iran.

RESUMEN

La Formación Kangan del Triásico Temprano es una sucesión mixta de carbonato-evaporita que se considera como parte del depósito de gas en carbonatos más grande en la región del Golfo Pérsico. Esta sucesión estratigráfica se caracteriza por una alternancia de caliza, dolomía, evaporitas y lutita,

que ha sido investigada en términos de las características de sus facies evaporíticas en la costa externa iraní. El cuerpo principal de los carbonatos Kangan fue depositado en una plataforma carbonatada restringida, de tipo rampa marina somera, y se sometió a una intensa diagénesis cerca de la superficie y ligeras modificaciones por sepultamiento. Las facies evaporíticas consisten de anhidrita primaria, anhidrita secundaria formada a partir de yeso y mezclas de carbonatos-evaporitas, predominantes en diferentes partes de la Formación Kangan y originadas por el clima árido y abruptos cambios eustáticos del nivel del mar. Este artículo se enfoca en las sucesiones evaporíticas, en las cuales se ha reconocido una serie de litofacies evaporíticas, que pueden clasificarse en dos grupos principales: (1) facies dominadas por carbonatos con contenido de evaporitas (facies tipo C), y (2) facies dominadas por evaporitas con contenido menor de carbonatos (facies tipo A). Son características comunes las láminas y bandas de anhidrita cristalina fina, evaporitas estratificadas (seudomorfos estratificados), seudomorfos de anhidrita intersticial formados a partir de yeso y anhidrita nodular. Las sucesiones evaporíticas a escala microscópica y macroscópica indican que la dolomitización y la precipitación de anhidrita tuvieron lugar simultáneamente, según los modelos de sabkha/filtraciones-reflujo. La sedimentación de evaporitas ocurrió, principalmente, en una cuenca costera en subsidencia de una laguna salina o hipersalina. En este contexto, la precipitación subacuática de las litofacies carbonatadas y evaporíticas fue seguida por el crecimiento intersticial de anhidrita diagenética. En su totalidad, la sucesión evaporítica refleja un proceso de relleno y procesos diagenéticos. El yeso se convirtió en seudomorfos de anhidrita en respuesta a eventos diagenéticos por sepultamiento somero a profundo.

Palabras clave: evaporitas, anhidrita, Formación Kangan, Triásico, Golfo Pérsico, Irán.

INTRODUCTION

A mixed evaporite-carbonate succession was deposited in the Persian Gulf area (Figure 1) during early Permian to Late Triassic period. The main part of the Early Triassic Kangan Formation ("Upper Khuff equivalent") is comprised of the above mentioned mixed strata. The pervasive carbonate ramp platform was established during Early to Late Triassic age, which was dominated by arid climate, maximum eustatic sea level falling and lack of any clastic inputs. These particular deposits overlie the carbonates of the Dalan Formation of early to late Permian age; on the other hand, the Kangan Formation is covered by the thick evaporite Dashtak succession of Late Triassic age (Figure 2). The collected evidence reveals that the evaporite facies involved direct deposition, secondary anhydrite pore filling and diagenetic anhydrite replacement, enhanced in the early to late diagenetic processes in the Kangan restricted carbonate platform (Lotfpour, 2005).

Much disagreement persists about interpreted depositional environments for ancient evaporites for several reasons: (1) Evaporite accumulation is not just a matter of deposition but also diagenesis (Warren, 2006). (2) Modern evaporitic depositional settings comparable to those in the rock record simply do not exist today (Kendall, 1984; Warren, 2006). (3) A considerable overlap in depositional textures is present for widely different depositional environments. (4) Diagenesis compromises the products of depositional processes; thus an analytical approach is required because evaporite deposits are highly susceptible to alterations that mask or completely obliterate primary textures. (5) Primary depositional textures (*e.g.*, anhydrite nodule generation) and secondary diagenetic fabrics (*i.e.*, gypsum transformed into anhydrite nodules) seemingly have identical appearances. (6) Diagenetic transformation pathways are not commonly preserved (Schreiber and El Tabakh, 2000) or well documented. The importance of these diagenetic processes on reservoir heterogeneity is widely recognized but the impact of dolomitization and anhydrite precipitation on the reservoir quality is a matter of debate (Lucia, 2007; Machel, 2005). This paper offers new insights into the evaporitic/carbonate lithofacies types encountered at two recently cored wells in the Persian Gulf, which provide a better understanding of the arid sedimentary environments during the Early Triassic period. The cored samples from these recent wells facilitate characterization of different types of evaporite facies that can be observed in this interval.

REGIONAL GEOLOGY

The Qatar arch, is a NNE-SSW trending positive tectonic feature of Precambrian origin, dividing the Persian Gulf into two troughs (the eastern and the western Hormuz Salt sub-basins). The structure of the arch was inherited from the Amar and Najd tectonic systems (Al-Husseini, 2000). Both, the arch and the adjacent troughs were rejuvenated and uplifted repeatedly since the early Silurian (Murris, 1980; Alsharhan and Nairn, 1997; Konert *et al.*, 2001; Pollastro, 2003). Tectonic movements during the Proterozoic–early Cambrian in central Saudi Arabia caused reactivation of pre-existing fault systems resulting in regional uplift, and may have gently elevated structural features including the Qatar arch (Al-Husseini, 2000; Murris, 1980). Both sub-basins were rejuvenated during the Silurian, resulting in the deposition of thin source-rock intervals (Bordenave, 2008). Thinning of Permian sediments may indicate the existence

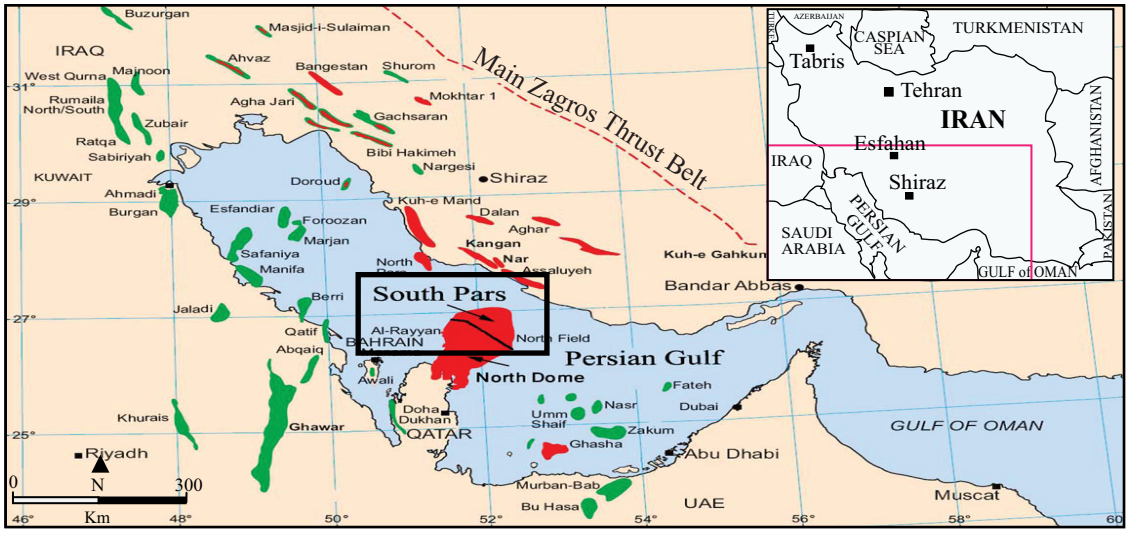

Figure 1. Geographical and geological setting of the study area. Main hydrocarbon fields in the Persian Gulf , adjacent areas and the Zagros thrust belt are shown (modified from Insalaco *et al.*, 2006).

of a depositional structural high southeast of the Zagros structure, or a block-faulted horst in the Qatar arch area (Kashfi, 1992). Post-Paleozoic tectonic activity may have revived this structural high, as indicated by the erosion of Late Triassic units (Murris, 1980; Kashfi, 1992). The arch was a positive structure during the Paleozoic and gradually subsided during the Jurassic (Saint-Marc, 1978). It was active periodically throughout the Mesozoic and including the late Cenozoic for sediments currently exposed at the surface (Konert, 2001; Alsharhan and Nairn, 1997).

The Early Triassic Kangan successions were deposited during restricted shallow-marine domination in the offshore area of the Persian Gulf (Figure 2). The general paleogeographic context of this system was a shallow marine setting with an inner platform that was very flat, ramp-like (Al-Jallal, 1987; Sharland *et al.,* 2001), but with local depressions (Figure 3). In the particular setting, where most of the mixed evaporite and carbonate facies types occur, depositional environments were prone to be restricted, with limited circulation due to high carbonate production and low accommodation potential (Insalaco *et al.*, 2006) (Figure 3).

MATERIALS AND METHODS

This study was based on a valid dataset consisting of core data, wireline logs and relevant thin sections that were obtained every 30 cm from cored intervals of the Kangan Formation, which is 160 m thick (the sum of cored interval is 340 m, as sampled by wells A and B). For facies analysis, the texture scheme of Dunham (1964) was used, together with observations made on sedimentary structures and fabrics, grain size, rock composition, and diagnostic allochems such as ooids, peloids and shells to help characterize the rocks. A petrographic study of the core samples, thin sections and scanning electron microscopy (SEM) was made

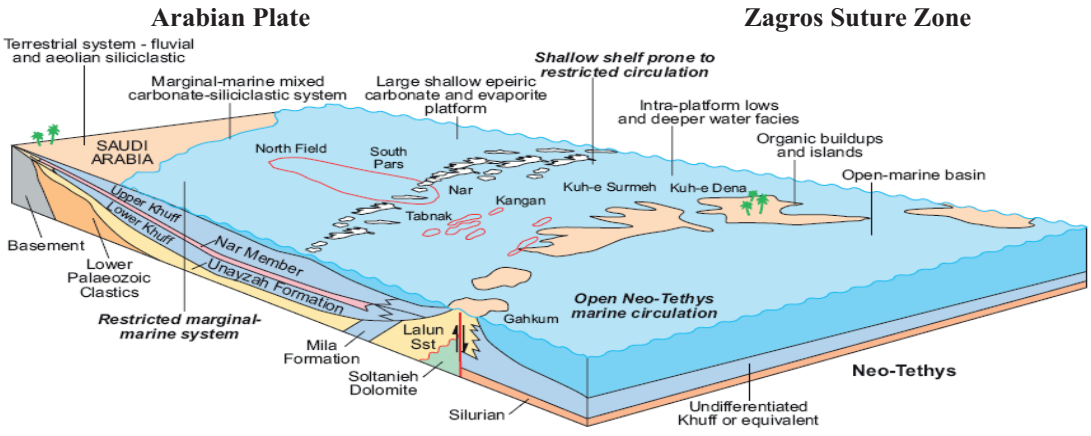

Figure 2. Schematic paleogeographical model of the Kangan platform system (Upper Khuff). Note that the field size is very small compared to the width of the facies tract. No vertical scale is implied (modified from Stampfli, 2000 and Sharland *et al.*, 2001).

to help discern facies types, and various diagenetic products. The study is mainly focused on the mixed evaporite/carbonate lithofacies of 117 m of the cored upper Kangan unit (Figure 4).

ROCK FACIES ANALYSIS

The carbonate and evaporite facies of the Kangan Formation can be classified into two groups:
1) Carbonate-dominated lithofacies with evaporite contents.
2) Evaporite-dominated lithofacies which is characterized by fine-grained and prismatic (lath) textures and granular textures.

Carbonate-dominated lithofacies with evaporite

This lithofacies is classified into three subgroups as follows:

C1- Mud-dominated carbonate

This mud-dominated carbonate lithofacies is heterogeneous in the reviewed core intervals, which is observed randomly in the K1 and K2 stratigraphic units. Massive to laminated mudstone to wackestone are common carbonate lithofacies with anhydrite content in the Kangan Formation (Figure 5a and Figure 6a, 6b and 6c). Sometimes, vertical burrows are present (Figure 6d), and no organic remains are embedded within these carbonate mudstone. There is a low anhydrite content, which is present as fine laminae, small nodules and recrystallized, equant crystals of about 3 mm in length (Figures 5b and 7a, 7b).

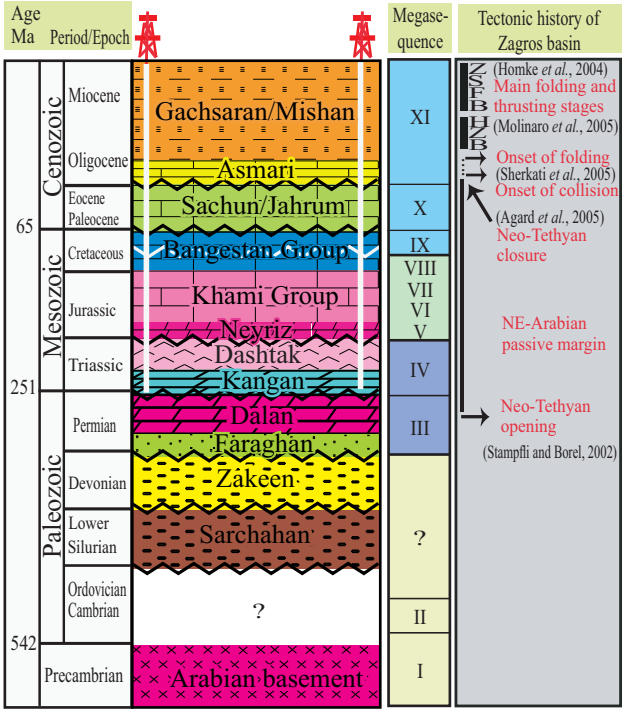

Figure 3. Generalized stratigraphy of the Persian Gulf showing lithostratigraphic units. The thickness of the stratigraphic column is approximately 4 km; it is dominated by shallow marine limestone, dolomite, shale and evaporite. Megasequences I-XI are after Alavi (2004). Not to scale.

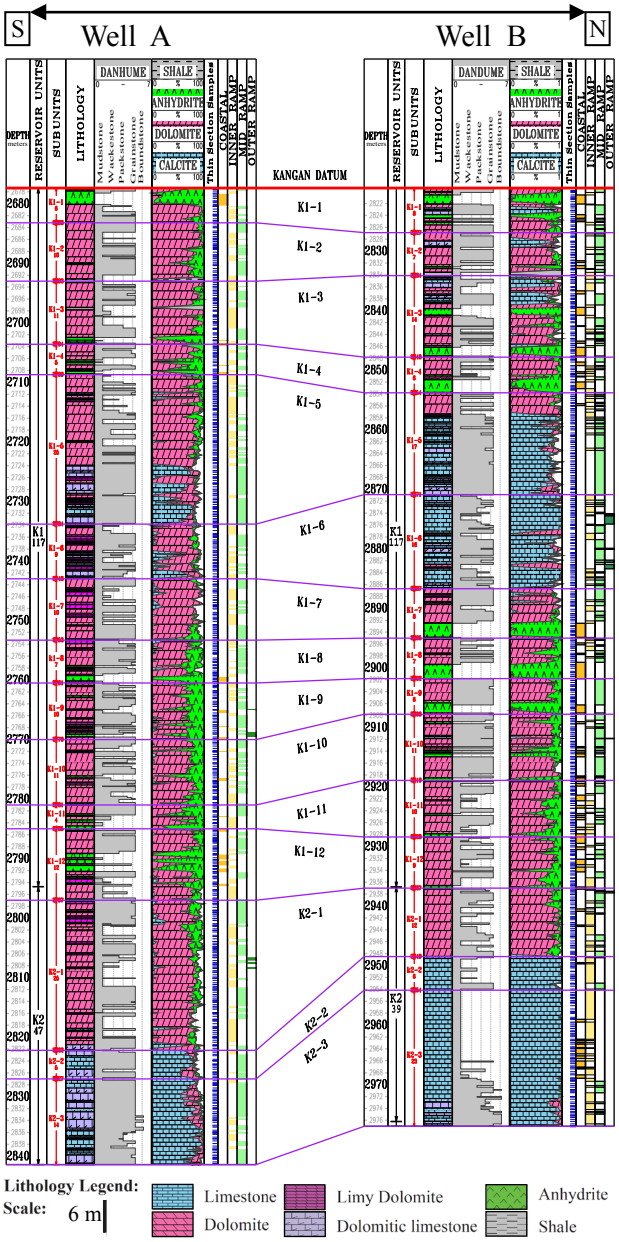

Figure 4. Stratigraphic correlation of the Kangan Formation in the study area.

C2- Alternation of carbonate and anhydrite laminae

This is an irregular alternation of carbonate and anhydrite laminae, where the thickness of each lamina oscillate from <1 mm to a few millimeters, and generally are less than 1 cm. The laminae are either even or deformed up to a certain degree, and small ripples are locally present (Figure 5c and Figure 7c). The relative proportion between

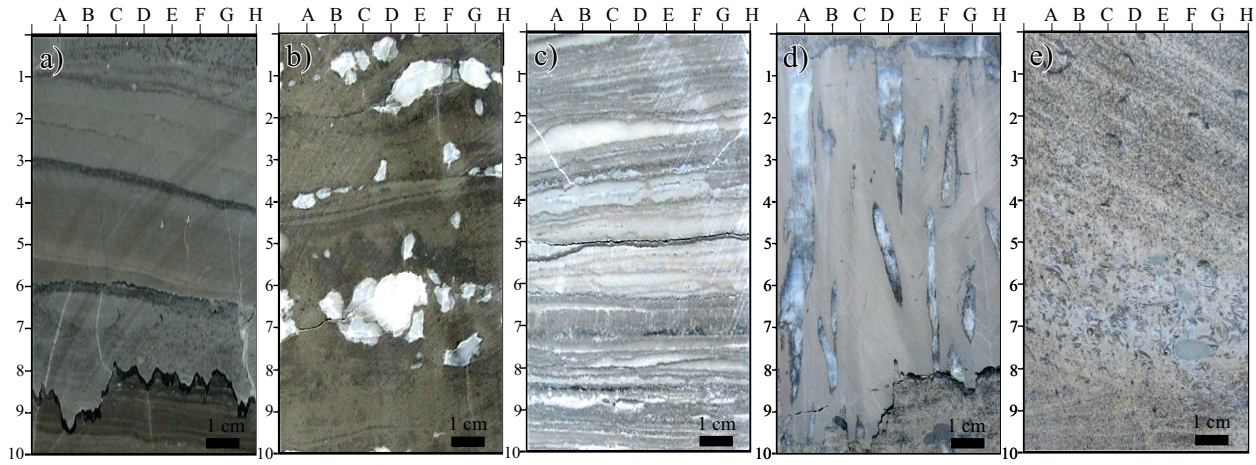

Figure 5. Carbonate lithofacies. a) Laminated carbonate mudstone. Some laminae are slightly deformed. Dark points correspond to millimeter-sized recrystallized, equant crystals of evaporate cast (1F). b) Laminated carbonate with anhydrite nodules (6D). c) Alternated laminated to wavy carbonate of mudstone (dark 1A), and anhydrite laminae (light 2B). d) Heavily bioturbated mud-supported facies; vertical burrows were filled by secondary anhydrite cement (G4). e) This grain-supported facies is characterized by patchy anhydrite cement (D7) and fine, skeletal debris (A6).

carbonate and anhydrite is variable, although carbonate usually predominates. Petrographic studies show that the presence of anhydrite pseudomorphs, after fine-grained gypsum crystals, is common. A few samples from the top of the borehole succession display clay-rich, dark laminae, that we speculate to be rich in organic matter (Figure 6c).

C3- Grain-dominated carbonate

Dolomitic/limy grainstone often with patchy or pervasive secondary anhydrite cementation is abundant, particularly in the lower Kangan Formation. The dolomitized ooid/oncoid and bioclastic grain-dominated facies generally includes medium to coarse-grained oncoids with secondary anhydrite cement and crystallized bioclastic grainstones where coated grains are common (Figure 5e and 7d). They often have significant amounts of shelly fragments (bivalves, forams, gastropods and calcareous algae), which are micritized (Figure 7e and 7f).These are oncoidal grainstones and occasionally packstones, mixed with microbial or peloidal debris that are predominantly observed in the K2 reservoir unit (Lotfpour, 2005).

Interpretation of carbonate-dominated lithofacies

Carbonates with evaporite lithofacies can be classified in terms of the main sedimentary settings as follows:

C1- The absence of burrowing and the low anhydrite content suggest that this lithofacies was deposited in a restricted environment with low sedimentation. The C1 lithofacies is assigned to a restricted lagoon.

C2- Two sedimentary environment interpretations can be postulated for the alternation of carbonate and anhydrite laminae:

a) The original alternation of carbonate and fine-crystalline gypsum laminae suggests distinct fluctuating conditions of precipitation.

b) Intertidal facies is characterized by dark laminae at the base of the succession, resembling the algal mats present in the intertidal belts of evaporitic environments.

C3- Grain-dominated lithofacies is interpreted as large tidal, sand wave complexes. The smaller bioclastic grainstone-packstone beds containing algae and foraminifera, with small bidirectional cross-beds and subhorizontal planar laminations are interpreted as shallow subtidal (lee-

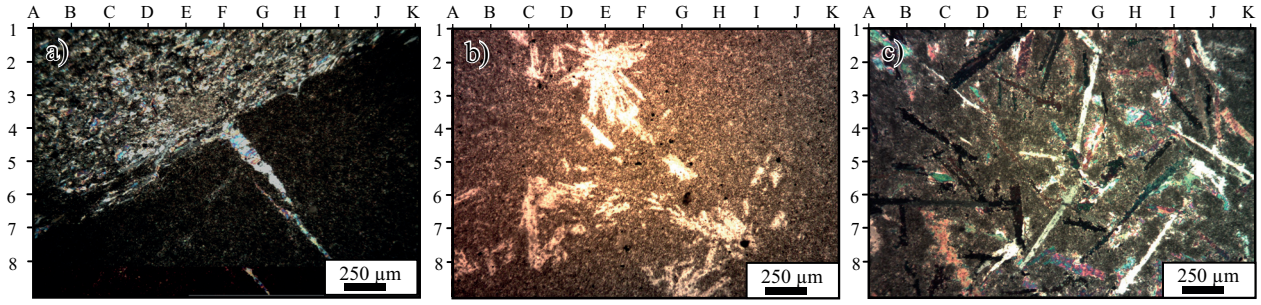

Figure 6. a) Dolomudstone with secondary anhydrite (D2), and a mud crack (G7). b) and c) Evaporite casts are present as needles of anhydrite (F3). Primary dolomite, as dolomicrite, was developed in this tide-dominated facies.

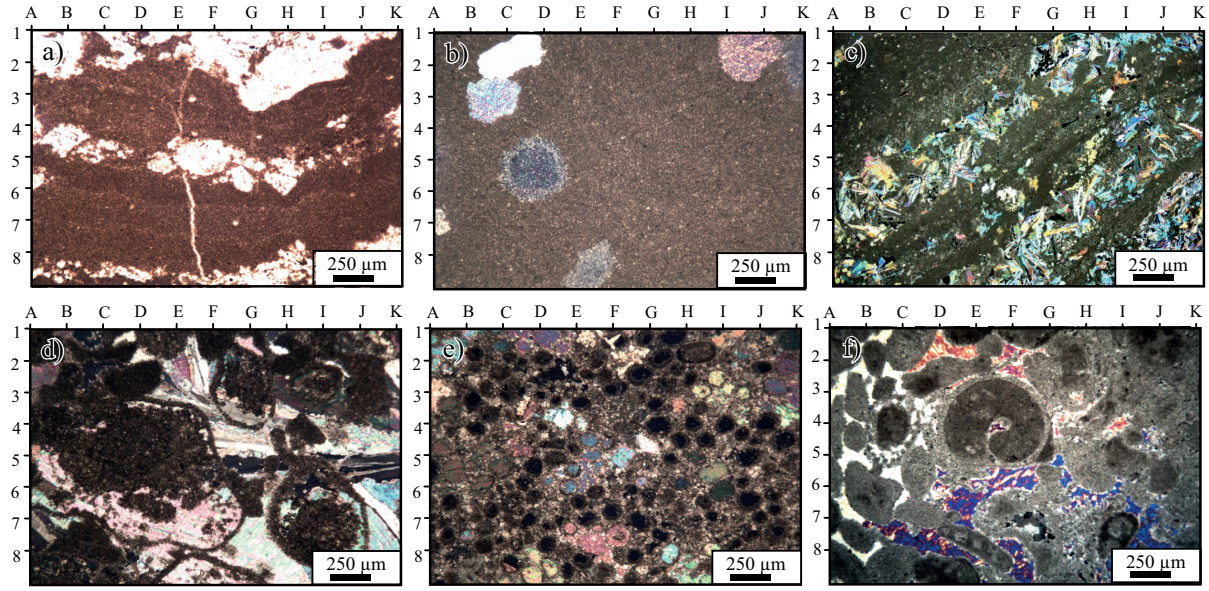

Figure 7. a) Alternation of carbonate laminae and evaporite nodules (G3); secondary anhydrite nodules (F5) and microfracture (E7) can also be developed in the hypersaline lagoonal setting. b) Anhydrite nodules (C3) within laminated dolomudstone that prevailed in lagoonal setting. c) Laminated to wave dolomudstone with anhydrite. d) Secondary anhydrite cement (E5) is common through this grain-supported facies; micritized oncoids (D5). e) Ooid grainstone; ooids were filled by secondary anhydrite (F5). f) Secondary anhydrite cement (E5) developed through this grain-supported facies.

ward shoals) to shoal sands, and are often associated with oncoidal packstones.

Anhydrite-dominated lithofacies

This lithofacies is classified into four subgroups as follows:

A1- Alternation of anhydrite and carbonate layers

This is an irregular alternation of anhydrite layers and scattered carbonate bands, where anhydrite layers predominate (Figure 8a). The individual thicknesses of these layers oscillate between a few centimeters to 1 m. The carbonate layers are massive to poorly laminated and mud-dominated, and are commonly thinner than the anhydrite layers. Grading occurs between this lithofacies and the alternation of carbonate just discussed before.

A2- Laminated to banded anhydrite

This lithofacies is made up of laminae and bands of anhydrite with scarce carbonate matrix. The individual bands attain a thickness of a few centimeters (Figure 8b). Under the microscope, many of these particles were identified as pseudomorphs after small gypsum crystals.

A3- Bedded pseudomorphs

This lithofacies consists of banded to bedded, vertically elongate anhydrite individuals (palisade fabric), suggesting a pseudomorphic origin after precursor evaporite crystals. The pseudomorphs are 1 to 30 cm long. The carbonate matrix is scarce and preferentially accumulated along the bedding planes. Bending or other deformation structures in the pseudomorphs are frequent, as are sutured boundaries between adjacent individuals (Figure 8c). In this lithofacies, a number of upward gradations were observed: (a) From the palisade fabric to other arrangements (oblique to bedding, sub-horizontal, random); (b) the crystal pseudomorphs to nodular morphologies; and (c) from bedded to interstitial pseudomorphs.

A4- Massive to nodular anhydrite

This general term is used here for a number of anhydrite lithofacies present in the samples, which exhibit gradations between them.

Massive anhydrite. This lithofacies consists of beds up to 1 m thick, where the anhydrite texture is microcrystalline and very pure. In detail, however, the presence of diffuse films of carbonate matrix suggests the existence of poorly-defined nodular to irregular masses, ranging from 1 to 10 cm in length (Figure 9a). In many samples, this lithofacies grades upward to better defined nodular forms.

Nodular anhydrite. This lithofacies is composed of nodules with variable morphologies: recumbent, palisade and aggregate, which occur either isolated or arranged in mosaic patterns. The diameter of the nodules oscillates from few millimeters to some centimeters, and the carbonate matrix is scarce (Figure 9a and 9b). This lithofacies has about 30 cm to 2 m in thickness.

Banded-nodular anhydrite. Bands and also beds up to 10 cm thick composed of anhydrite nodules are found in these cores. The diameter of the nodules oscillates between 1 and 10 cm, and is rarely <0.5 cm. Enterolithic (contorted) layers of nodular anhydrite was observed (Figure 9c).

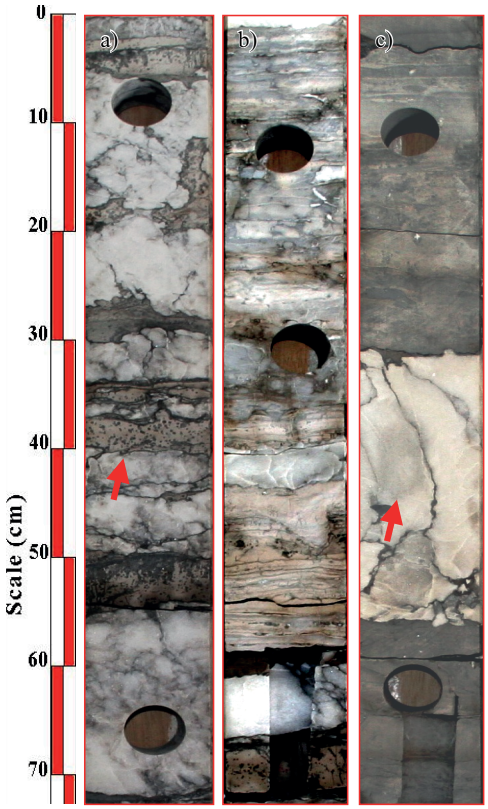

Figure 8. Anhydrite lithofacies: bedded pseudomorphs. a) and b) Bedded anhydrite pseudomorphs after selenitic gypsum displaying a palisade fabric. Plastic deformation and sutured contacts between the pseudomorphs (red arrows) are seen. c) Detail of the bedded pseudomorphs. Carbonate matrix (dark material) is locally abundant. Vertically elongated anhydrite individuals (palisade fabric) with sutured contact between the pseudomorphs are seen.

Graded-nodular anhydrite. In this lithofacies, the size of nodules decreases upward, from some centimeters at the base to <0.1 cm at the top, and the nodules are often slightly flattened (Figures 9e). The thickness of anhydrite levels displaying this lithofacies varies from 5 to 20 cm.

Interpretation of anhydrite-dominated lithofacies

In the A1 and A2 lithofacies, where anhydrite pseudomorphs after precursor gypsum can be petrographically identified, the various types of anhydrite laminae and bands can be interpreted as precursor gypsum deposits composed of small-sized crystals. As in C2 lithofacies, the original alternation of gypsum and carbonate bands (lithofacies A1) suggests fluctuating conditions of precipitation on a shallow depositional floor. In the laminated to banded anhydrite lithofacies (A2), the micronodular texture of anhydrite locally present could be assigned, *a priori*, to interstitial precipitation in a supratidal setting (sabkha). It is assumed that the precursor fine-grained gypsum in the laminae and bands was formed subaqueously in a restricted subtidal setting, and the micronodular textures were formed during the subsequent diagenetic transformation of the gypsum crystals into anhydrite (see below).The bedded pseudomorphs (lithofacies A3) presumably correspond to selenite gypsum. At present, such crystals are known to grow subaqueously with competitive fabrics on shallow depositional floors (Warren, 2006).

Some of the massive to nodular anhydrite lithofacies (A4) were formed in exposed conditions as in the case of the recent anhydrite in the supratidal flats of the Persian Gulf (Sharland, 2006). However, the absence of enterolithic layers in the samples (a typical feature of the vadose-capillary zone), suggests that for some nodular growths other different settings cannot be ruled out. In this lithofacies there is no evidence for an origin by replacement of a precursor fabric of graded selenite. Presumably, this lithofacies was formed in the sabkha setting at the top of the phreatic zone under the control of a salinity gradient (an upward increase of concentration) in the brine.

BRECCIAS

Carbonate-dominated breccias

The massive anhydrite and brecciated dolomudstone in the upper Kangan Formation is interpreted as a collapse breccia originated by the partial dissolution of intervening evaporites and carbonates during significant surface exposure (Figure 10a). Dolomitic clasts between 1 to 5 cm in length are irregularly distributed in this lithofacies (Figures 10b and 10c). Gradation between these breccias and undisturbed carbonate mudstones are observed in the core interval. In some samples, the presence of secondary anhydrite clasts is also recorded as well as fibrous anhydrite veins cementing the dolomitic clasts. A late diagenetic origin is suggested for this lithofacies because of anhydrite dissolution during the exhumation.

Carbonate-anhydrite breccias

This lithofacies, made up of thin levels of carbonate-anhydrite breccias intercalated into other lithofacies, is not common. In these scarce levels, anhydrite clasts display a number of morphologies such as angular clasts, nodules, and pseudomorphs. The carbonate clasts may exhibit soft sediment deformation (Figures 10d and 10e), suggesting unlithified sediment conditions at the time of brecciation. A synsedimentary origin is proposed for this lithofacies because of early exposure and dissolution of gypsum/anhydrite.

Observations on carbonate brecciation

Regardless of the local existence of gravity-driven, sedimentary breccias (Giner, 1978, 1980), the brecciation process has often been assigned to the dissolution of

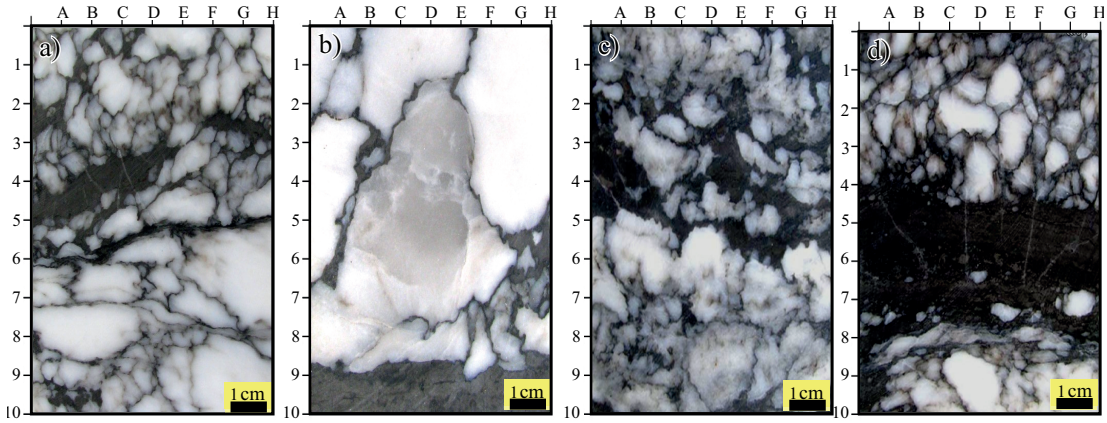

Figure 9. Anhydrite lithofacies. a) Bedded pseudomorphs after selenitic gypsum. b) This facies includes anhydrite with sutured contacts between the pseudomorphs (C2). c) and d) Details of the bedded pseudomorphs.

evaporite beds and to the collapse of both, the associated carbonate and the carbonate layers overlying the evaporite beds. The discussion, however, is mainly focused on the timing of the brecciation process. However, we assume an early diagenetic origin linked to synsedimentary exposure (Bordonaba and Aurell, 2002; Bordonaba, 2003). These breccias usually contain secondary, recrystallized, equant crystals of gypsum derived from the hydration of recrystallized, equant crystals of anhydrite present in the carbonate lithofacies throughout the borehole interval. This recrystallized, equant crystals of anhydrite, which were interpreted as formed during moderate to deep burial diagenesis, clearly preceded the brecciation process. On the other hand, the boundary between the top of the anhydrite rocks and the overlying carbonate breccias constitute a regional aquifer of paramount importance. All of these observations suggest that groundwater was a major factor in sulphate dissolution and associated carbonate brecciation in the region during the final exhumation of the lowermost Kangan carbonate series.

EVAPORITE CYCLICITY

The observed pattern clearly reflects the existence of cycles (Figure 10a). Only one type of these cycles seems to represent a sabkha succession in a carbonate tidal complex (Figure 10a). The rest exhibit shallowing upward successions originally involving gypsum precipitated subaqueously: fine-grained gypsum (banded anhydrite) grading to nodular anhydrite (Figure 10b); bedded selenite (bedded pseudomorphs) grading to nodular anhydrite (Figure 11c); and interstitial selenite (interstitial pseudomorphs) grading to nodular anhydrite (Figure 10d). Kasprzyk (2003) described the shallow water facies association, which is

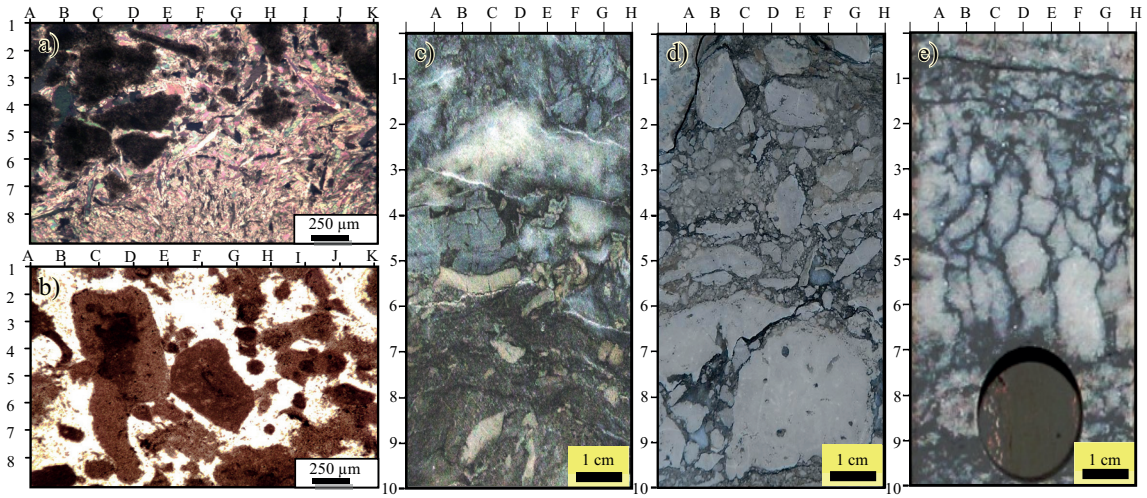

Figure 10. Carbonate-anhydrite brecciated lithofacies. a) Large anhydrite nodule (H6) is present among the brecciated mudstone (C3) to wackestone that can be seen particularly at the base. b) Brecciated dolomudstone (C4) with secondary anhydrite plugging (G6). c) Dolomitic clasts (D5) between 1 to 5 cm in length and the brecciated mudstone (C4) are irregularly distributed in this lithofacies. d) Brecciated fenestral mudstone (D8) with secondary anhydrite plugging (B5). e) The anhydrite nodules and brecciated dolomudstone in this facies is interpreted as a solution collapse due to partial dissolution of intervening evaporite and carbonate. There is an increasing occurrence of laminated mudstone, anhydrite nodules and small brecciated levels.

related to an evaporative inner platform/lagoon system. Taking these cycles together, an "ideal" cycle for the Kangan Formation can be proposed, which would comprise up to seven lithofacies of a shallowing upward cycle (Figure 10b). Some of these cycles, however, are just irregular alternations and only contain two or three lithofacies. Other cycles are better developed and involve up to four or five lithofacies; these latter cycles would represent a closer approximation to the ideal cycle.

A distinction between a lower cyclic assemblage and an upper cyclic assemblage can be made (Figure 10). The lower assemblage is composed of individual cycles with a total thickness of ~40 m. This assemblage is characterized by cycles beginning with carbonate lithofacies (K2), followed by fine-grained gypsum and bedded anhydrite, and ending with massive to nodular anhydrite at the top. In general, the anhydrite tops are not very thick and may display graded-nodular lithofacies. The upper cyclic assemblage is made up of individual cycles with a total thickness of ~117 m (K1). This assemblage is characterized by cycles with carbonate lithofacies, and an absence of laminated to banded, fine-crystalline anhydrite.

ANHYDRITIZATION MODEL

The most outstanding evaporite lithofacies are interpreted as peritidal deposits with laminated to banded fine-crystalline anhydrite; bedded carbonates bear a strong resemblance to the evaporite facies currently characterizing the precipitation in the evaporative salinas. In these shallow settings, the fine-crystalline anhydrite facies always precipitate at lower salinities than gypsum. Moreover, the gypsum is preferentially developed in the salinas where the hydrologic circuits are active throughout the year. Similarly, the evaporitic basin of the Kangan unit in the study area can be interpreted as a subsiding coastal basin of the salina or lagoon type, where the thin beds of gypsum (<10 cm) suggest a shallow setting. The massive to nodular anhydrite forming the top of the shallowing upward cycles is interpreted as a synsedimentary, sabkha condition during the deposition.

Anhydritization from early diagenesis to moderate burial diagenesis

Two aspects of interpretative significance emerge from the observation of the pseudomorphic lithofacies A3: The plastic deformation of the evaporites took place within a soft (unlithified) carbonate matrix; and the progressive, upward gradation from geometric to nodular morphologies apparently occurred as a continuous process. As for the first aspect, the plastic deformation of the pseudomorphs, especially in the palisade fabric, can be assigned to the gypsum-to-anhydrite conversion involving a decrease in volume. Despite the fact that the plastic behavior of the evaporite during their alteration to carbonates is compatible with early diagenesis, the marked deformation recorded in the pseudomorphs suggests shallow to moderate burial conditions of the deposit (Figure 12). As for the second aspect, it is worth noting that, in the upward morphological gradation (pseudomorphic to nodular), sharp boundaries or erosive contacts were not observed as would be expected if subaerial exposure at the top of each cycle had been the main factor of the anhydritization process. All these observations suggest that the anhydritization of carbonates were a continuous process that started under synsedimentary conditions in contact with sabkha brines, and continued during shallow to moderate burial in contact with interstitial, pore brines (Figure 12).

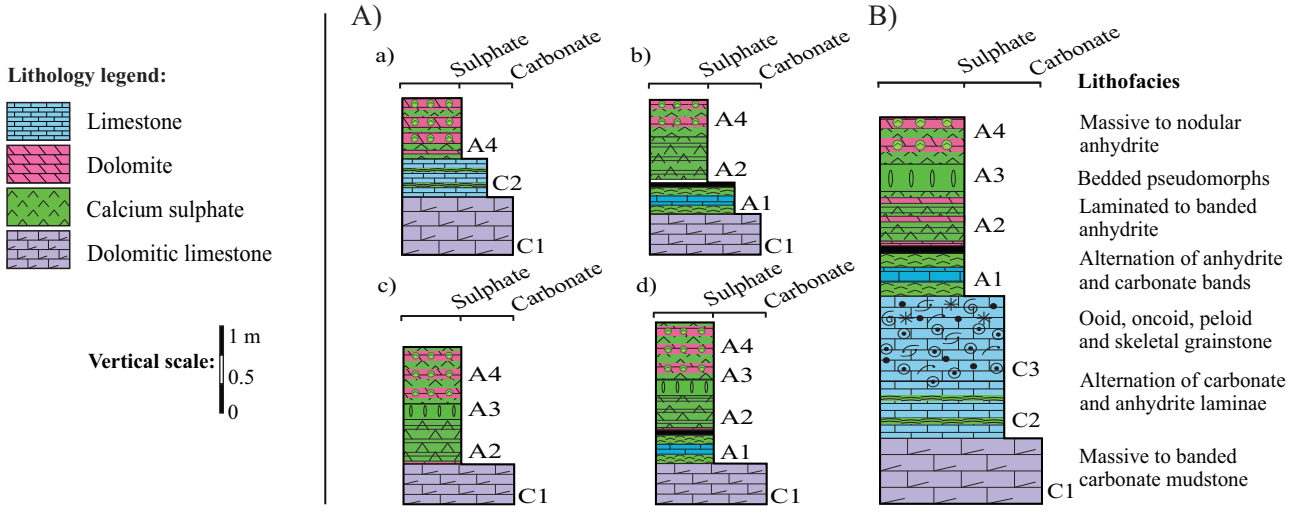

Figure 11. Evaporitic cycles of the Kangan Formation. A) Individual cycles. a) Sabkha cycle; b) Fine-crystalline laminated to banded anhydrite lithofacies grading to nodular anhydrite; c) Bedded selenite (bedded pseudomorphic lithofacies) grading to nodular anhydrite; d) Interstitial evaporite grading to nodular anhydrite. B) Evaporitic lithofacies succession.

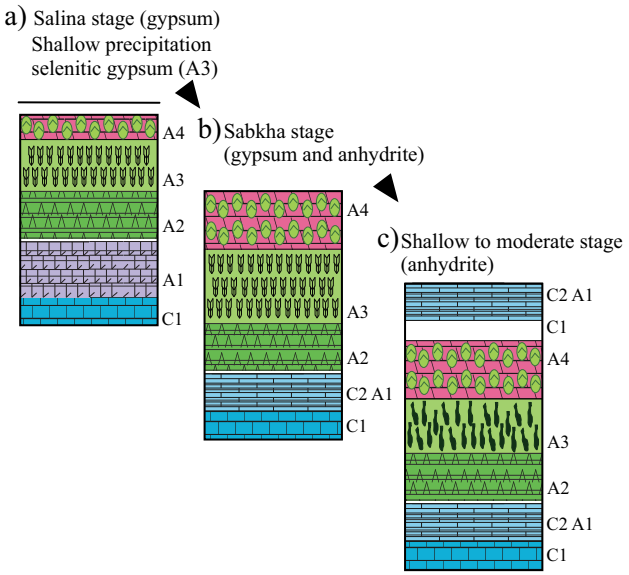

Figure 12. Schematic evolution of the two (pseudomorphic) selenite lithofacies present at the Kangan Formation. The evolution is presented as a continuous process accomplished along three successive stages: a) Salina stage: subaqueous precipitation of the bedded evaporite. b) Sabkha stage (at the top of the cycle): nodular growth of anhydrite and initiation of the anhydritization and deformation of the underlying selenite. c) Shallow to moderate burial stage: anhydritization and advanced deformation (by compaction) of the selenite. Lithofacies C1 to A4 as in Figure 11.

Anhydritization from moderate to deep burial diagenesis

A case of late (burial) diagenetic anhydrite is represented by the recrystallized, equant crystals embedded in the massive to banded carbonate mudstone (lithofacies C1), which are distributed throughout the core interval of the borehole. Presumably, they were formed from interstitial brines during moderate to deep burial diagenesis.

ANHYDRITE TEXTURE TYPES

The Triassic Kangan Formation includes diverse anhydrite cements that involve important processes developed in layered, poikilotopic, pore filling and pervasive, nodular and sparse crystals, fracture filling and veinlet forms. These textures were completed during different diagenetic stages, by replacement, displacement and pore occludin at different degrees, and affected the reservoir quality in the Kangan Formation.

The particular morphologies are consistent with deposition taking place a few millimeter from the depositional surface by displacive intrasediment growth of crystals beneath the brine from supersaturated pore fluids in the capillary and/or upper phreatic zone (*e.g.*, Kerr and Thomson, 1963; Warren, 2000). Anhydrite layer fabric, massive fabric, and nodule fabric display different textures (Figure 13) that include sparse and isolated crystals, acicular or needle shape texture, equant to mosaic texture, fibrous parallel to subparallel texture, fibrous radial texture, felted to aphanitic texture, lath shape crystals texture and combination texture (Table 1).

ANHYDRITIZATION AND RESERVOIR QUALITY

The reservoir quality of Kangan Formation depends on the vertical and lateral facies variations, affected by early diagenetic processes, depth of burial and regional tectonics. The described anhydrite layers with variable thicknesses divide the Kangan reservoir body into two reservoir intervals: the lower Kangan (K2) and the upper Kangan (K1) with different reservoir quality characteristics. In addition, anhydrite pore-filling dissolution with variable dimensions has increased secondary porosity and improved the reservoir quality. However, evaporite deposits have reduced the

Table 1. Paragenetic sequence of different anhydrite textures in the upper Kangan Formation.

Diagenetic events	**Diagenetic environments**			**Remark**
Common / Less common	Meteoric diagenetic	Moderate diagenetic	Deep burial diagenetic	
Scattered evaporite crystals	■			Tidal flat anhydrite and gypsum
Anhydrite nodules	■	▪		More relation to sabkha depositional environment; impact of pore brine water
Anhydrite layer	■			Probably primary gypsum was deposited from saline water in a sabkha environment setting
Evaporite veins		■		Primary gypsum nodules are formed as a result of hydration
Poikilotopic anhydrite	▪	■	■	Texture with anhydrite dispersed within pores and also as replacement in the dolomite
Pervasive anhydrite		■		Large crystals with a uniform expansion that filled pores in the grain-supported facies
Anhydrite pore filling		■	■	Anhydrite pore filling, with large crystals in fractures

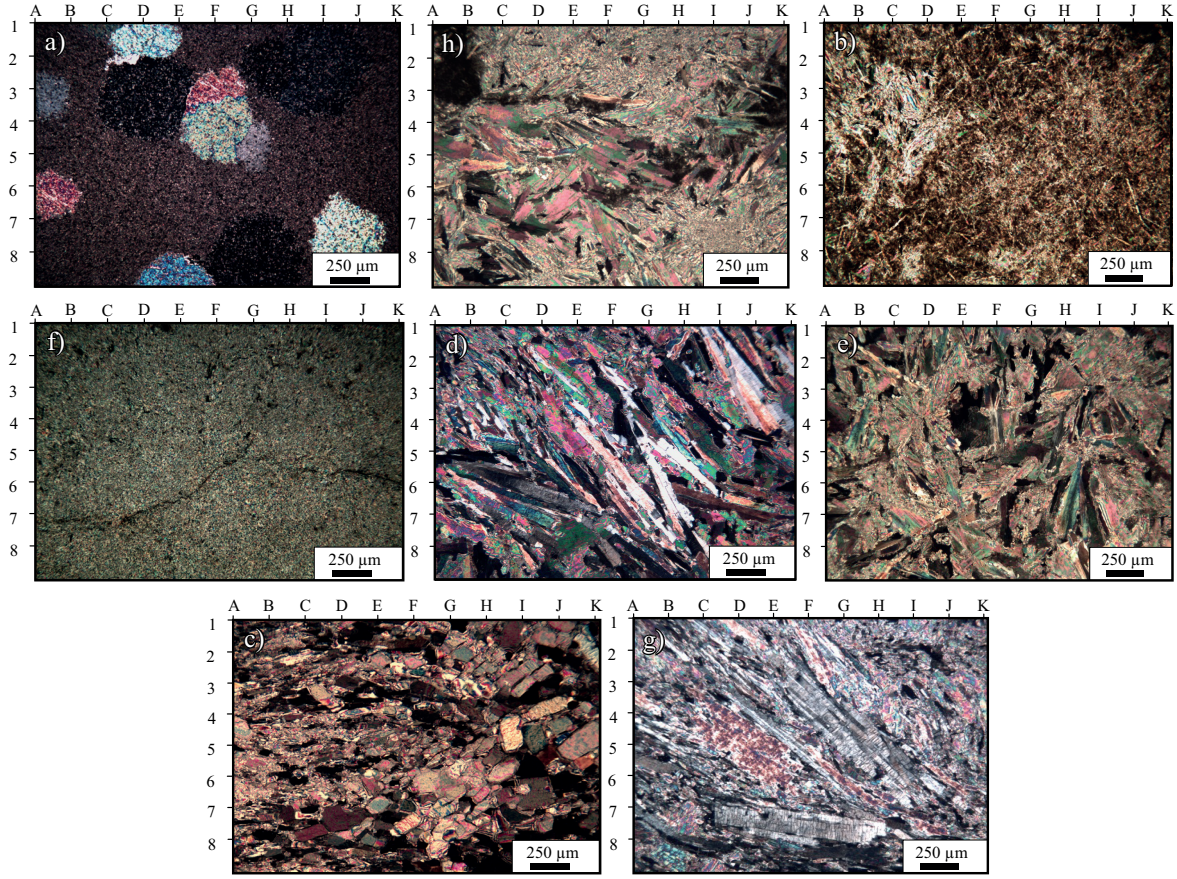

Figure 13. Different textures of the evaporites of the Kangan Formation exposed in the study area. a) Isolated crystals, b) acicular or needle shape texture, c) equant to mosaic texture, d) fibrous parallel to subparallel texture, e), fibrous radial texture, f) felted to aphanitic texture, g) lath shape crystals texture, and h) and combination texture.

reservoir quality properties in most of the upper Kangan unit (Insalaco *et al.*, 2006). Evaluation of reservoir quality in various intervals indicates that secondary dolomitization in the absence of anhydrite precipitation or with only patchy anhydrite has enhanced the reservoir quality. Where anhydrite cement is pervasive and has plugged the rock fabric, reservoir characteristics have significantly decreased.

This study indicates that the poikilotopic and pervasive anhydrite cements have the greatest impact in reducing reservoir quality. Secondary anhydrite cement that filled the intercrystalline voids, has decreased the porosity and permeability in the Kangan Formation.

CONCLUSIONS

1) The evaporitic succession of the Kangan Formation in the Persian Gulf region, up to 160 m thick, exhibits a number of individual cycles. An "ideal" cycle of this succession is made up of massive to banded carbonate lithofacies at the base, fine-crystalline anhydrite lithofacies in the central part, and nodular anhydrite at the top. This is a shallowing upward cycle that starts with subaqueous precipitation of carbonate and evaporites and ends with the subaerial growth of anhydrite.

2) A number of depositional cycles are deduced, and a lower and upper assemblage can be differentiated. In the upper assemblage, the cycles are thinner on average than in the lower assemblage, but display less diversified lithofacies and reflect shallower settings, which are characterized by the deposition of carbonate-rich, interstitial evaporite.

3) The relevant sedimentary cycles coincide with a wide range of distinctive sedimentary environments including sabkha, arid tidal flat, coastal salina or hypersaline lagoon with domination of eustatic sea level changes.

4) The primary anhydrite sedimentation has a close relationship with dolomite precipitation in the sedimentary basin, which is followed by different secondary anhydritization processes including anhydrite replacement and pore filling/plugging.

5) In the upper Kangan unit, the anhydrite lithofacies initiated a conversion into evaporites under syn-sedimentary conditions including contact with sabkha brines. Subsequently, the process continued during shallow to moderate burial diagenesis in contact with interstitial (pore) brines.

ACKNOWLEDGEMENTS

The authors thank the experts and management of POGC (Pars Oil and Gas Company of Iran), who provided financial support for this research, and data preparation; they also gave permission to publish this paper. We express our thanks to Islamic Azad University, North Tehran authorities. We are grateful to Dr. Peter Birkle for the editorial handling of the manuscript, and to David M. Steinhauff and three anonymous reviewers for the constructive comments.

REFERENCES

Agard, P., Omrani, J., Jolivet, L., Mouthereau, F., 2005, Convergence history across Zagros(Iran): constraints from collisional and earlier deformation: International Journal of Earth Sciences, doi 10.1007/s00531-005-0481-4.

Alavi, M., 2004, Regional stratigraphy of the Zagros Fold-Thrust Belt of Iran and its proforeland evolution: American Journal of Science, 304, 1-20.

Al-Husseini, M.I., 2000, Origin of the Arabian Plate Structures: Amar Collision and Najd Rift: GeoArabia, 5, 527-542.

Al-Jallal, I.A., 1987, Diagenetic effect on reservoir properties of the Permian Khuff Formation in Eastern Saudi Arabia: Presentation at the Fifth Middle East Oil show, Society of Petroleum Engineers, Bahrain, SPE, 745, 465-475.

Alsharhan, A.S., Nairn, A.E.M., 1997, Sedimentary basins and petroleum geology of the Middle East: Amsterdam, Elsevier, 843 pp.

Bordenave, M.L., 2008, The origin of the Permo-Triassic gas accumulations in the Iranian Zagros foldbelt and contiguous offshore area: a review of the Paleozoic petroleum system: Journal of Petroleum Geology, 31, 3-42.

Bordonaba, A.P., 2003, Evolución sedimentaria del Jurásico Inferior (Hettangiense – Pliensbachiense) en el sector centroriental de la Cordillera Ibérica: Zaragoza, España, Universidad de Zaragoza, Tesis Doctoral, 417 pp.

Bordonaba, A.P., Aurell, M., 2002, Variación lateral de facies del Jurásico basal de la Cordillera Ibérica Central: origen diagenético temprano y tectónica sedimentaria: Acta Geologica Hispanica, 37, 355-368.

Dunham, R.J., 1964, Classification of carbonate rocks according to depositional texture, *in* Ham, W.E. (ed.), Classification of carbonate rocks: American Association of Petroleum Geologists Memoir, 1, 108-121.

Giner, J., 1978, Origen y significado de las brechas del Lías de la Mesa de Prades (Tarragona): Estudios Geológicos, 34, 529-533.

Giner, J., 1980. Estudio sedimentológico y diagenético de las facies carbonatadas del Jurásico de los Catalónides, Maestrazgo y Rama Aragonesa de la Cordillera Ibérica: Barcelona, España, Universidad de Barcelona, tesis doctoral, 315 p.

Homke, S.J., Vergés, J., Garcés, M., Emami, H., Karpuz, R., 2004. Magnetostratigraphy of Miocene–Pliocene Zagros foreland deposits in the front of the Push-e Kush Arc (Lurestan Province, Iran): Earth and Planetary Science Letters, 225, 397–410.

Insalaco, E., Virgone, A., Courme, B., Gaillot, J., Kamali, M., Moallemi A., Lotfpour M., Monibi S., 2006, Upper Dalan Member and Kangan Formation between the Zagros Mountains and offshore Fars, Iran: depositional system, biostratigraphy and stratigraphic architecture: GeoArabia, 11, 75-176.

Kashfi, M.S., 1992, Geology of the Permian super-giant gas reservoirs in the greater Persian Gulf area: Journal of Petroleum Geology, 15(4), 465-480.

Kasprzyk, A., 2003, Sedimentological and diagenetic patterns of anhydrite deposits in the Badenian evaporite basin of the Carpathian Fore deep, southern Poland: Sedimentary Geology, 158, 167-194.

Kendall, A.C., 1984, Evaporites: Geoscience Canada, Reprint Series, 1, 259-296.

Kerr, S.D., Thompson, A., 1963, Origin of nodular and bedded anhydrite in Permian shelf sediments, Texas and New Mexico: American Association of Petroleum Geologist Bulletin, 47, 1726-1732.

Konert, G., Afif, A.M., Al-Hajari, S.A., Droste, H., 2001, Palaeozoic stratigraphy and hydrocarbon habitat of the Arabian Plate: GeoArabia, 6, 407-442.

Lotfpour, M., 2005, Microfacies, biostratigraphy and sequence stratigraphy of the Kangan and Dalan formations in the Zagros Basin: Tehran, Shahid Beheshti University, doctoral dissertation, 550 p.

Lucia, F.J., 2007, Carbonate reservoir characterisation: an integrated approach: New York, Springer, 2nd. edition, 336 p.

Machel, H.G., 2005, Investigations of burial diagenesis in carbonate hydrocarbon reservoir rocks: Geoscience Canada, 32, 103-128.

Molinaro, M., Leturmy, P., Guezou, J.C., de Lamotte, D.F., Eshraghi, S.A., 2005, The structure and kinematics of the southeastern Zagros fold-thrustbelt, Iran: From thin-skinned to thick-skinned tectonics: Tectonics, TC3007, doi:10.1029/2004TC001633.

Murris, R.J., 1980, The Middle East: stratigraphic evolution and oil habitat: American Association of Petroleum Geologists Bulletin, 64, 597-618.

Pollastro, R.M., 2003, Total Petroleum Systems of the Palaeozoic and Jurassic, Greater Ghawar Uplift and Adjoining Provinces of Central Saudi Arabia and Northern Arabian-Persian Gulf: United States Geological Survey Bulletin, 2202-H. <http://pubs.usgs.gov/bul/b2202-h/>.

Saint-Marc, E., 1978, Arabian Peninsula, *in* Moullade, M. and Nairn, A.E.M. (eds.), The Phanerozoic geology of the world II: The Mesozoic: Amsterdam, Elsevier, 435-462.

Schreiber, B.S., El Tabakh, M., 2000, Deposition and early alteration of evaporites: Sedimentary Geology, 47, 215-238.

Sherkati, S., Molinaro, M., Frizon de Lamotte, D., Letouzey, J., 2005, Detachment folding in the Central and Eastern Zagros fold-belt (Iran): salt mobility, multiple detachments and late basement control: Journal of Structural Geology, 27, 1680-1696.

Sharland, P.R., Archer, R., Casey, D.M., Davies, R.B., Hall, S.H., Heward, A.P., Horbury, A.D., Simmons, M.D., 2001, Arabian Plate Sequence Stratigraphy: GeoArabia Special Publication, 2, 371 pp.

Stampfli, G., 2000, Tethyan Oceans, *in* Bozkurt, E., Winchester, J.A., Piper, J.D.A (eds.), Tectonics and Magmatism in Turkey and the Surrounding Area: The Geological Society Special Publication, 173, 1-23.

Stampfli, G.M., Borel, G.D., 2002. A plate tectonic model for the Paleozoic and Mesozoic constrained by dynamic plate boundaries and restored synthetic oceanic isochrons: Earth and Planetary Science Letters, 196, 17-33.

Testa, G., Lugli, S., 2000, Gypsum anhydrite transformation in messinian evaporites of central Tuscany (Italy): Sedimentary Geology, 130(3), 249-268.

Warren, J., 2000, Dolomite: occurrence, evolution and economically important associations: Earth-Science Reviews, 52, 1-81.

Warren, J.K., 2006, Evaporites: Sediments, Resources and Hydrocarbons: Berlin, Springer-Verlag, , 1035 pp.

Manuscript received: November 18, 2012
Corrected manuscript received: June 3, 2013
Manuscript accepted: July 31, 2013